MIT Libraries | DSpace@MIT

MIT Open Access Articles

Study of CP Asymmetry in B[superscript 0]–[bar over B][superscript 0] Mixing with Inclusive Dilepton Events

Massachusetts Institute of Technology

Study of *CP* Asymmetry in B^0-$\bar{B}^0$ Mixing with Inclusive Dilepton Events

J. P. Lees,[1] V. Poireau,[1] V. Tisserand,[1] E. Grauges,[2] A. Palano,[3a,3b] G. Eigen,[4] B. Stugu,[4] D. N. Brown,[5] L. T. Kerth,[5] Yu. G. Kolomensky,[5] M. J. Lee,[5] G. Lynch,[5] H. Koch,[6] T. Schroeder,[6] C. Hearty,[7] T. S. Mattison,[7] J. A. McKenna,[7] R. Y. So,[7] A. Khan,[8] V. E. Blinov,[9a,9b,9c] A. R. Buzykaev,[9a] V. P. Druzhinin,[9a,9b] V. B. Golubev,[9a,9b] E. A. Kravchenko,[9a,9b] A. P. Onuchin,[9a,9b,9c] S. I. Serednyakov,[9a,9b] Yu. I. Skovpen,[9a,9b] E. P. Solodov,[9a,9b] K. Yu. Todyshev,[9a,9b] A. J. Lankford,[10] M. Mandelkern,[10] B. Dey,[11] J. W. Gary,[11] O. Long,[11] C. Campagnari,[12] M. Franco Sevilla,[12] T. M. Hong,[12] D. Kovalskyi,[12] J. D. Richman,[12] C. A. West,[12] A. M. Eisner,[13] W. S. Lockman,[13] W. Panduro Vazquez,[13] B. A. Schumm,[13] A. Seiden,[13] D. S. Chao,[14] C. H. Cheng,[14] B. Echenard,[14] K. T. Flood,[14] D. G. Hitlin,[14] T. S. Miyashita,[14] P. Ongmongkolkul,[14] F. C. Porter,[14] M. Röhrken,[14] R. Andreassen,[15] Z. Huard,[15] B. T. Meadows,[15] B. G. Pushpawela,[15] M. D. Sokoloff,[15] L. Sun,[15] P. C. Bloom,[16] W. T. Ford,[16] A. Gaz,[16] J. G. Smith,[16] S. R. Wagner,[16] R. Ayad,[17,a] W. H. Toki,[17] B. Spaan,[18] D. Bernard,[19] M. Verderi,[19] S. Playfer,[20] D. Bettoni,[21a] C. Bozzi,[21a] R. Calabrese,[21a,21b] G. Cibinetto,[21a,21b] E. Fioravanti,[21a,21b] I. Garzia,[21a,21b] E. Luppi,[21a,21b] L. Piemontese,[21a] V. Santoro,[21a] A. Calcaterra,[22] R. de Sangro,[22] G. Finocchiaro,[22] S. Martellotti,[22] P. Patteri,[22] I. M. Peruzzi,[22,b] M. Piccolo,[22] M. Rama,[22] A. Zallo,[22] R. Contri,[23a,23b] M. Lo Vetere,[23a,23b] M. R. Monge,[23a,23b] S. Passaggio,[23a] C. Patrignani,[23a,23b] E. Robutti,[23a] B. Bhuyan,[24] V. Prasad,[24] A. Adametz,[25] U. Uwer,[25] H. M. Lacker,[26] P. D. Dauncey,[27] U. Mallik,[28] C. Chen,[29] J. Cochran,[29] S. Prell,[29] H. Ahmed,[30] A. V. Gritsan,[31] N. Arnaud,[32] M. Davier,[32] D. Derkach,[32] G. Grosdidier,[32] F. Le Diberder,[32] A. M. Lutz,[32] B. Malaescu,[32,c] P. Roudeau,[32] A. Stocchi,[32] G. Wormser,[32] D. J. Lange,[33] D. M. Wright,[33] J. P. Coleman,[34] J. R. Fry,[34] E. Gabathuler,[34] D. E. Hutchcroft,[34] D. J. Payne,[34] C. Touramanis,[34] A. J. Bevan,[35] F. Di Lodovico,[35] R. Sacco,[35] G. Cowan,[36] J. Bougher,[37] D. N. Brown,[37] C. L. Davis,[37] A. G. Denig,[38] M. Fritsch,[38] W. Gradl,[38] K. Griessinger,[38] A. Hafner,[38] K. R. Schubert,[38] R. J. Barlow,[39,d] G. D. Lafferty,[39] R. Cenci,[40] B. Hamilton,[40] A. Jawahery,[40] D. A. Roberts,[40] R. Cowan,[41] G. Sciolla,[41] R. Cheaib,[42] P. M. Patel,[42,e] S. H. Robertson,[42] N. Neri,[43a] F. Palombo,[43a,43b] L. Cremaldi,[44] R. Godang,[44,f] P. Sonnek,[44] D. J. Summers,[44] M. Simard,[45] P. Taras,[45] G. De Nardo,[46a,46b] G. Onorato,[46a,46b] C. Sciacca,[46a,46b] M. Martinelli,[47] G. Raven,[47] C. P. Jessop,[48] J. M. LoSecco,[48] K. Honscheid,[49] R. Kass,[49] E. Feltresi,[50a,50b] M. Margoni,[50a,50b] M. Morandin,[50a] M. Posocco,[50a] M. Rotondo,[50a] G. Simi,[50a,50b] F. Simonetto,[50a,50b] R. Stroili,[50a,50b] S. Akar,[51] E. Ben-Haim,[51] M. Bomben,[51] G. R. Bonneaud,[51] H. Briand,[51] G. Calderini,[51] J. Chauveau,[51] Ph. Leruste,[51] G. Marchiori,[51] J. Ocariz,[51] M. Biasini,[52a,52b] E. Manoni,[52a] S. Pacetti,[52a,52b] A. Rossi,[52a] C. Angelini,[53a,53b] G. Batignani,[53a,53b] S. Bettarini,[53a,53b] M. Carpinelli,[53a,53b,g] G. Casarosa,[53a,53b] A. Cervelli,[53a,53b] M. Chrzaszcz,[53a] F. Forti,[53a,53b] M. A. Giorgi,[53a,53b] A. Lusiani,[53a,53c] B. Oberhof,[53a,53b] E. Paoloni,[53a,53b] A. Perez,[53a] G. Rizzo,[53a,53b] J. J. Walsh,[53a] D. Lopes Pegna,[54] J. Olsen,[54] A. J. S. Smith,[54] R. Faccini,[55a,55b] F. Ferrarotto,[55a] F. Ferroni,[55a,55b] M. Gaspero,[55a,55b] L. Li Gioi,[55a] A. Pilloni,[55a,55b] G. Piredda,[55a] C. Bünger,[56] S. Dittrich,[56] O. Grünberg,[56] M. Hess,[56] T. Leddig,[56] C. Voß,[56] R. Waldi,[56] T. Adye,[57] E. O. Olaiya,[57] F. F. Wilson,[57] S. Emery,[58] G. Vasseur,[58] F. Anulli,[59,h] D. Aston,[59] D. J. Bard,[59] C. Cartaro,[59] M. R. Convery,[59] J. Dorfan,[59] G. P. Dubois-Felsmann,[59] W. Dunwoodie,[59] M. Ebert,[59] R. C. Field,[59] B. G. Fulsom,[59] M. T. Graham,[59] C. Hast,[59] W. R. Innes,[59] P. Kim,[59] D. W. G. S. Leith,[59] P. Lewis,[59] D. Lindemann,[59] S. Luitz,[59] V. Luth,[59] H. L. Lynch,[59] D. B. MacFarlane,[59] D. R. Muller,[59] H. Neal,[59] M. Perl,[59,e] T. Pulliam,[59] B. N. Ratcliff,[59] A. Roodman,[59] A. A. Salnikov,[59] R. H. Schindler,[59] A. Snyder,[59] D. Su,[59] M. K. Sullivan,[59] J. Va'vra,[59] W. J. Wisniewski,[59] H. W. Wulsin,[59] M. V. Purohit,[60] R. M. White,[60,i] J. R. Wilson,[60] A. Randle-Conde,[61] S. J. Sekula,[61] M. Bellis,[62] P. R. Burchat,[62] E. M. T. Puccio,[62] M. S. Alam,[63] J. A. Ernst,[63] R. Gorodeisky,[64] N. Guttman,[64] D. R. Peimer,[64] A. Soffer,[64] S. M. Spanier,[65] J. L. Ritchie,[66] A. M. Ruland,[66] R. F. Schwitters,[66] B. C. Wray,[66] J. M. Izen,[67] X. C. Lou,[67] F. Bianchi,[68a,68b] F. De Mori,[68a,68b] A. Filippi,[68a] D. Gamba,[68a,68b] L. Lanceri,[69a,69b] L. Vitale,[69a,69b] F. Martinez-Vidal,[70] A. Oyanguren,[70] P. Villanueva-Perez,[70] J. Albert,[71] Sw. Banerjee,[71] A. Beaulieu,[71] F. U. Bernlochner,[71] H. H. F. Choi,[71] G. J. King,[71] R. Kowalewski,[71] M. J. Lewczuk,[71] T. Lueck,[71] I. M. Nugent,[71] J. M. Roney,[71] R. J. Sobie,[71] N. Tasneem,[71] T. J. Gershon,[72] P. F. Harrison,[72] T. E. Latham,[72] H. R. Band,[73] S. Dasu,[73] Y. Pan,[73] R. Prepost,[73] and S. L. Wu[73]

(*BABAR* Collaboration)

[1]*Laboratoire d'Annecy-le-Vieux de Physique des Particules (LAPP), Université de Savoie, CNRS/IN2P3, F-74941 Annecy-Le-Vieux, France*
[2]*Universitat de Barcelona, Facultat de Fisica, Departament ECM, E-08028 Barcelona, Spain*
[3a]*INFN Sezione di Bari, I-70126 Bari, Italy*
[3b]*Dipartimento di Fisica, Università di Bari, I-70126 Bari, Italy*

[4]University of Bergen, Institute of Physics, N-5007 Bergen, Norway

[5]Lawrence Berkeley National Laboratory and University of California, Berkeley, California 94720, USA

[6]Ruhr Universität Bochum, Institut für Experimentalphysik 1, D-44780 Bochum, Germany

[7]University of British Columbia, Vancouver, British Columbia, Canada V6T 1Z1

[8]Brunel University, Uxbridge, Middlesex UB8 3PH, United Kingdom

[9a]Budker Institute of Nuclear Physics SB RAS, Novosibirsk 630090, Russia

[9b]Novosibirsk State University, Novosibirsk 630090, Russia

[9c]Novosibirsk State Technical University, Novosibirsk 630092, Russia

[10]University of California at Irvine, Irvine, California 92697, USA

[11]University of California at Riverside, Riverside, California 92521, USA

[12]University of California at Santa Barbara, Santa Barbara, California 93106, USA

[13]University of California at Santa Cruz, Institute for Particle Physics, Santa Cruz, California 95064, USA

[14]California Institute of Technology, Pasadena, California 91125, USA

[15]University of Cincinnati, Cincinnati, Ohio 45221, USA

[16]University of Colorado, Boulder, Colorado 80309, USA

[17]Colorado State University, Fort Collins, Colorado 80523, USA

[18]Technische Universität Dortmund, Fakultät Physik, D-44221 Dortmund, Germany

[19]Laboratoire Leprince-Ringuet, Ecole Polytechnique, CNRS/IN2P3, F-91128 Palaiseau, France

[20]University of Edinburgh, Edinburgh EH9 3JZ, United Kingdom

[21a]INFN Sezione di Ferrara, I-44122 Ferrara, Italy

[21b]Dipartimento di Fisica e Scienze della Terra, Università di Ferrara, I-44122 Ferrara, Italy

[22]INFN Laboratori Nazionali di Frascati, I-00044 Frascati, Italy

[23a]INFN Sezione di Genova, I-16146 Genova, Italy

[23b]Dipartimento di Fisica, Università di Genova, I-16146 Genova, Italy

[24]Indian Institute of Technology Guwahati, Guwahati, Assam 781 039, India

[25]Universität Heidelberg, Physikalisches Institut, D-69120 Heidelberg, Germany

[26]Humboldt-Universität zu Berlin, Institut für Physik, D-12489 Berlin, Germany

[27]Imperial College London, London SW7 2AZ, United Kingdom

[28]University of Iowa, Iowa City, Iowa 52242, USA

[29]Iowa State University, Ames, Iowa 50011-3160, USA

[30]Physics Department, Jazan University, Jazan 22822, Kingdom of Saudi Arabia

[31]Johns Hopkins University, Baltimore, Maryland 21218, USA

[32]Laboratoire de l'Accélérateur Linéaire, IN2P3/CNRS et Université Paris-Sud 11, Centre Scientifique d'Orsay,
F-91898 Orsay Cedex, France

[33]Lawrence Livermore National Laboratory, Livermore, California 94550, USA

[34]University of Liverpool, Liverpool L69 7ZE, United Kingdom

[35]Queen Mary, University of London, London E1 4NS, United Kingdom

[36]University of London, Royal Holloway and Bedford New College, Egham, Surrey TW20 0EX, United Kingdom

[37]University of Louisville, Louisville, Kentucky 40292, USA

[38]Johannes Gutenberg-Universität Mainz, Institut für Kernphysik, D-55099 Mainz, Germany

[39]University of Manchester, Manchester M13 9PL, United Kingdom

[40]University of Maryland, College Park, Maryland 20742, USA

[41]Massachusetts Institute of Technology, Laboratory for Nuclear Science, Cambridge, Massachusetts 02139, USA

[42]McGill University, Montréal, Québec, Canada H3A 2T8

[43a]INFN Sezione di Milano, I-20133 Milano, Italy

[43b]Dipartimento di Fisica, Università di Milano, I-20133 Milano, Italy

[44]University of Mississippi, University, Mississippi 38677, USA

[45]Université de Montréal, Physique des Particules, Montréal, Québec, Canada H3C 3J7

[46a]INFN Sezione di Napoli, I-80126 Napoli, Italy

[46b]Dipartimento di Scienze Fisiche, Università di Napoli Federico II, I-80126 Napoli, Italy

[47]NIKHEF, National Institute for Nuclear Physics and High Energy Physics, NL-1009 DB Amsterdam, Netherlands

[48]University of Notre Dame, Notre Dame, Indiana 46556, USA

[49]Ohio State University, Columbus, Ohio 43210, USA

[50a]INFN Sezione di Padova, I-35131 Padova, Italy

[50b]Dipartimento di Fisica, Università di Padova, I-35131 Padova, Italy

[51]Laboratoire de Physique Nucléaire et de Hautes Energies, IN2P3/CNRS, Université Pierre et Marie Curie-Paris6,
Université Denis Diderot-Paris7, F-75252 Paris, France

[52a]INFN Sezione di Perugia, I-06123 Perugia, Italy

[52b]Dipartimento di Fisica, Università di Perugia, I-06123 Perugia, Italy

[53a]INFN Sezione di Pisa, I-56127 Pisa, Italy

^{53b}*Dipartimento di Fisica, Università di Pisa, I-56127 Pisa, Italy*

^{53c}*Scuola Normale Superiore di Pisa, I-56127 Pisa, Italy*

^{54}*Princeton University, Princeton, New Jersey 08544, USA*

^{55a}*INFN Sezione di Roma, I-00185 Roma, Italy*

^{55b}*Dipartimento di Fisica, Università di Roma La Sapienza, I-00185 Roma, Italy*

^{56}*Universität Rostock, D-18051 Rostock, Germany*

^{57}*Rutherford Appleton Laboratory, Chilton, Didcot, Oxon OX11 0QX, United Kingdom*

^{58}*CEA, Irfu, SPP, Centre de Saclay, F-91191 Gif-sur-Yvette, France*

^{59}*SLAC National Accelerator Laboratory, Stanford, California 94309 USA*

^{60}*University of South Carolina, Columbia, South Carolina 29208, USA*

^{61}*Southern Methodist University, Dallas, Texas 75275, USA*

^{62}*Stanford University, Stanford, California 94305-4060, USA*

^{63}*State University of New York, Albany, New York 12222, USA*

^{64}*Tel Aviv University, School of Physics and Astronomy, Tel Aviv 69978, Israel*

^{65}*University of Tennessee, Knoxville, Tennessee 37996, USA*

^{66}*University of Texas at Austin, Austin, Texas 78712, USA*

^{67}*University of Texas at Dallas, Richardson, Texas 75083, USA*

^{68a}*INFN Sezione di Torino, I-10125 Torino, Italy*

^{68b}*Dipartimento di Fisica, Università di Torino, I-10125 Torino, Italy*

^{69a}*INFN Sezione di Trieste, I-34127 Trieste, Italy*

^{69b}*Dipartimento di Fisica, Università di Trieste, I-34127 Trieste, Italy*

^{70}*IFIC, Universitat de Valencia-CSIC, E-46071 Valencia, Spain*

^{71}*University of Victoria, Victoria, British Columbia, Canada V8W 3P6*

^{72}*Department of Physics, University of Warwick, Coventry CV4 7AL, United Kingdom*

^{73}*University of Wisconsin, Madison, Wisconsin 53706, USA*

(Received 10 November 2014; published 25 February 2015)

We present a measurement of the asymmetry A_{CP} between same-sign inclusive dilepton samples $\ell^+\ell^+$ and $\ell^-\ell^-$ ($\ell = e, \mu$) from semileptonic B decays in $\Upsilon(4S) \to B\bar{B}$ events, using the complete data set recorded by the *BABAR* experiment near the $\Upsilon(4S)$ resonance, corresponding to 471×10^6 $B\bar{B}$ pairs. The asymmetry A_{CP} allows comparison between the mixing probabilities $\mathcal{P}(\bar{B}^0 \to B^0)$ and $\mathcal{P}(B^0 \to \bar{B}^0)$, and therefore probes CP and T violation. The result, $A_{CP} = [-3.9 \pm 3.5(\text{stat}) \pm 1.9(\text{syst})] \times 10^{-3}$, is consistent with the standard model expectation.

A neutral B meson can transform to its antiparticle through the weak interaction. A difference between the probabilities $\mathcal{P}(\bar{B}^0 \to B^0)$ and $\mathcal{P}(B^0 \to \bar{B}^0)$ is allowed by the standard model (SM) and is a signature of violations of both CP and T symmetries. This type of CP violation, called CP violation in mixing, was first observed in the neutral kaon system [1], but has not been observed in the neutral B system, where the SM predicts an asymmetry of the order of 10^{-4} [2]. The current experimental average of CP asymmetry in mixing measured in the B^0 system alone is $A_{CP} = (+2.3 \pm 2.6) \times 10^{-3}$ [3], dominated by the *BABAR* [4,5], D0 [6], and Belle [7] experiments. The most recent LHCb result, $A_{CP} = (-0.2 \pm 1.9 \pm 3.0) \times 10^{-3}$ [8], had not been included in the aforementioned average. A recent measurement in a mixture of B^0 and B_s^0 mesons by the D0 Collaboration deviates from the SM expectation by more than 3 standard deviations [9]. Improving the experimental precision is crucial for understanding the source of this apparent discrepancy.

The neutral B meson system can be described by an effective Hamiltonian $\mathbf{H} = \mathbf{M} - i\Gamma/2$ for the two states $|B^0\rangle$ and $|\bar{B}^0\rangle$. Assuming CPT symmetry, the mass eigenstates can be written as $|B_{L/H}\rangle = p|B^0\rangle \pm q|\bar{B}^0\rangle$. If $|q/p| \neq 1$, both CP and T symmetries are violated. Details of the formalism can be found in Refs. [10,11].

The $B^0\bar{B}^0$ pair created in the $\Upsilon(4S)$ decay evolves coherently until one B meson decays. In this analysis, we use the charge of the lepton (electron or muon) in semileptonic B decays to identify the flavor of the B meson at the time of its decay. If the second B meson has oscillated to its antiparticle, it will produce a lepton that has the same charge as the lepton from the first B decay. The CP asymmetry A_{CP} between $\mathcal{P}(\bar{B}^0 \to B^0)$ and $\mathcal{P}(B^0 \to \bar{B}^0)$ can be measured by the charge asymmetry of the same-sign dilepton event rate $\mathcal{P}_{\ell\ell}^{\pm\pm}$:

$$A_{CP} = \frac{\mathcal{P}_{\ell\ell}^{++} - \mathcal{P}_{\ell\ell}^{--}}{\mathcal{P}_{\ell\ell}^{++} + \mathcal{P}_{\ell\ell}^{--}} = \frac{1 - |q/p|^4}{1 + |q/p|^4}. \qquad (1)$$

This asymmetry is independent of the B decay time.

We present herein an updated measurement of A_{CP} using inclusive dilepton events collected by the *BABAR* detector at the PEP-II asymmetric-energy e^+e^- storage rings at

SLAC National Accelerator Laboratory. The data set consists of 471×10^6 $B\bar{B}$ pairs produced at the $\Upsilon(4S)$ resonance peak (on peak) and 44 fb^{-1} of data collected at a center-of-mass (c.m.) energy 40 MeV below the peak (off peak) [12]. Monte Carlo (MC) simulated $B\bar{B}$ events equivalent to 10 times the data set based on EVTGEN [13] and GEANT4 [14] with full detector response and event reconstruction are used to test the analysis procedure. The main changes with respect to the previous BABAR analysis [4] include doubling the data set, a higher signal selection efficiency, improved particle identification algorithms, and a time-independent approach instead of a time-dependent analysis.

The BABAR detector is described in detail elsewhere [15]. Events are selected if the two highest-momentum particles in the event are consistent with the electron or muon hypotheses. All quantities are evaluated in the c.m. frame unless stated otherwise. The higher-momentum and lower-momentum lepton candidates are labeled as 1 and 2, respectively. Four lepton combinations are allowed, $\ell_1\ell_2 = \{ee, e\mu, \mu e, \mu\mu\}$, as are four charge combinations, for a total of 16 subsamples. We assume e-μ universality, i.e., equal A_{CP} for all $\ell_1\ell_2$ combinations. The time-integrated signal yields can be written as [16]

$$N_{\ell_1\ell_2}^{\pm\pm} = \frac{1}{2}N_{\ell_1\ell_2}^0(1 \pm a_{\ell_1} \pm a_{\ell_2} \pm A_{CP})\chi_d^{\ell_1\ell_2}, \quad (2)$$

$$N_{\ell_1\ell_2}^{\pm\mp} = \frac{1}{2}N_{\ell_1\ell_2}^0(1 \pm a_{\ell_1}\mp a_{\ell_2})(1 - \chi_d^{\ell_1\ell_2} + r_B), \quad (3)$$

in the limit of $A_{CP} \ll 1$ and $a_{\ell_j} \ll 1$, where $a_{\ell_j} = (\epsilon_{\ell_j}^+ - \epsilon_{\ell_j}^-)/(\epsilon_{\ell_j}^+ + \epsilon_{\ell_j}^-)$ is the average charge asymmetry of the detection efficiency for lepton j, r_B is the B^+/B^0 event ratio, $\chi_d^{\ell_1\ell_2}$ is the effective mixing probability of neutral B mesons including efficiency corrections, and $N_{\ell_1\ell_2}^0$ is the neutral B signal yield for the $\ell_1\ell_2$ flavor combination.

A small fraction of the background comes from $e^+e^- \to f\bar{f}(\gamma)$ continuum events ($f \in \{u, d, s, c, e, \mu, \tau\}$). This contribution is subtracted using the off-peak data and the integrated luminosity ratio [12] between the on-peak and off-peak data sets. The remaining background comes from $B\bar{B}$ events, where at least one lepton candidate originates from $B \to X \to \ell Y$ cascade decays, or from a hadron misidentified as a lepton.

Including the background, we expand Eqs. (2) and (3) to parametrize the total observed numbers of events as

$$M_{\ell_1\ell_2}^{\pm\pm} = \frac{1}{2}N_{\ell_1\ell_2}^0(1 + R_{\ell_1\ell_2}^{\pm\pm})\left[1 \pm a_{\ell_1} \pm a_{\ell_2} \pm \frac{1 + \delta_{\ell_1\ell_2}R_{\ell_1\ell_2}^{\pm\pm}}{1 + R_{\ell_1\ell_2}^{\pm\pm}}A_{CP}\right]\chi_d^{\ell_1\ell_2}, \quad (4)$$

$$M_{\ell_1\ell_2}^{\pm\mp} = \frac{1}{2}N_{\ell_1\ell_2}^0(1 + R_{\ell_1\ell_2}^{\pm\mp})(1 \pm a_{\ell_1}\mp a_{\ell_2})(1 - \chi_d^{\ell_1\ell_2} + r_B), \quad (5)$$

where $R_{\ell_1\ell_2}^{\pm\pm}$ and $R_{\ell_1\ell_2}^{\pm\mp}$ are background-to-signal ratios under the condition $A_{CP} = 0$, and $\delta_{\ell_1\ell_2}$ is the probability of a same-sign background event being consistent with the flavors of the neutral B pairs at the time of their decay after B^0-$\bar{B}^0$ mixing, i.e., $\ell^+\ell^+$ ($\ell^-\ell^-$) for B^0B^0 ($\bar{B}^0\bar{B}^0$), minus the probability of the opposite case, i.e., $\ell^+\ell^+$ ($\ell^-\ell^-$) for $\bar{B}^0\bar{B}^0$ (B^0B^0). The detailed derivation can be found in the Supplemental Material [16]. For the opposite-sign events, signal is CP symmetric. The background originating from B^0B^0 ($\bar{B}^0\bar{B}^0$) preferably contributes to $\ell^+\ell^-$ ($\ell^-\ell^+$) because a primary lepton tends to have a higher momentum than a cascade lepton. Therefore, the background yield is also a function of A_{CP}. However, the coefficient of A_{CP} is less than 0.01 for the final data sample, so it is ignored in the fits.

Events with ≥ 1 lepton (single-lepton sample) are used to constrain the charge asymmetry of the detector efficiency $a_\ell \equiv (a_{\ell_1} + a_{\ell_2})/2$. The inclusive single-lepton asymmetry a_{on} in on-peak data can be expressed as [16]

$$a_{on} = \alpha + \beta\chi_d A_{CP} + \gamma a_\ell, \quad (6)$$

where parameters α, β, and γ are functions of the following quantities: the fractions and asymmetries of the continuum background, misidentified leptons, and cascade leptons; the B^0/B^+ ratio; and $w_{B^0}^{casc}$ the probability of the cascade lepton's charge incorrectly identifying the B flavor at the time of the B decay.

We build a χ^2 fit using the $8 + 8 + 1$ equations represented by Eqs. (4)–(6) to extract A_{CP}. For the single-lepton sample, we use only electrons since the purity is much higher than that of muons.

The event selection requires ≥ 4 charged particle tracks and the normalized second-order Fox-Wolfram moment [17] $R_2 < 0.6$. The leptons should satisfy $0.6 < p_{\ell_2} \leq p_{\ell_1} < 2.2$ GeV. The polar angle θ of the electron (muon) candidate in the laboratory frame is required to satisfy $-0.788 < \cos\theta < 0.961$ ($-0.755 < \cos\theta < 0.956$). The lepton is rejected if, when combined with another lepton of opposite charge, the invariant mass is consistent with that of a J/ψ or a $\psi(2S)$ meson, or the kinematics is consistent with a photon conversion. The lepton tracks must pass a set of quality requirements. For dilepton events, the invariant mass of the lepton pair must be greater than 150 MeV. The

proper decay time difference Δt of the two B mesons can be determined from the distance along the collision axis between the points of closest approach of the lepton tracks to the beam spot and the boost factor ($\simeq 0.56$) of the c.m. frame. We require $|\Delta t| < 15$ ps and its uncertainty $\sigma_{\Delta t} < 3$ ps.

Electrons and muons are identified by two separate multivariate algorithms that predominately use the shower shape and energy deposition in the electromagnetic calorimeter for electrons and the track path length and cluster shape in the instrumented flux return for muons. The electron (muon) identification efficiency is approximately 93% (40%–80% depending on momentum). The probability of a hadron being identified as an electron (muon) is $< 0.1\%$ ($\sim 1\%$).

To further suppress background, we use random forest multivariate classifiers [18]. Off-peak data are used to represent continuum events, and simulated events are used for signal and $B\bar{B}$ background. In the dilepton sample, we use six variables: p_{ℓ_1}, p_{ℓ_2}, thrust and sphericity [19] of the rest of the event, the opening angle θ_{12} of the two tracks in the c.m. frame, and Δt. Separate classifiers are trained on the same-sign and opposite-sign samples. The ee, $e\mu$, μe, and $\mu\mu$ samples are also trained separately. The dilepton signal probability distributions of the classifiers are shown in Fig. 1. We select events with a probability > 0.7 to minimize the statistical uncertainty based on fits to the $B\bar{B}$ MC sample. The final on-peak data sample includes 2.5% continuum background for all dilepton samples, and 35%

(8%) $B\bar{B}$ background in the same-sign (opposite-sign) sample.

Approximately 0.1% (3%) of selected electrons (muons) in dilepton samples are misidentified. According to the simulation, nearly 98% of the misidentified electrons come from pions and 87% (12%) of the misidentified muons come from pions (kaons). To correct for the difference in the muon misidentification rates between data and MC samples, we study the muon identification efficiency in clean kaon and pion control samples from the process $D^{*+} \to D^0 (\to K^- \pi^+) \pi^+$ (and the charge-conjugate process). The ratios of the efficiencies between data and MC samples are used to scale the misidentified muon component in the MC sample. The correction to μ^+ (μ^-) is 0.792 ± 0.012 (0.797 ± 0.013). Since the misidentification rate is very low for electrons, we use a much larger pion control sample from $K_s^0 \to \pi^+ \pi^-$ decays. This control sample has a lower momentum spectrum and does not cover the region of $p > 2.5$ GeV in the laboratory frame, which accounts for less than 8% of the misidentified leptons. The correction to misidentified e^+ (e^-) is 1.00 ± 0.10 (0.56 ± 0.10). The quoted uncertainties are conservative estimates that result from mismatched momentum spectra and from a small fraction of kaons and protons among misidentified electrons.

For the single-lepton sample, the random forest algorithm uses the number of tracks, the event thrust, R_2, the difference between the observed energy in the event and the sum of the $e^+ e^-$ beam energies, the cosines of the angles between the lepton and the axes of the thrust and the sphericity of the rest of the event, and the zeroth-order and second-order polynomial moments L_0 and L_2, where $L_n = \sum p_i (\cos \theta_i)^n$, p_i is the momentum of a particle in the rest of the event and θ_i is the angle between that particle and the single-lepton candidate. We optimize the selection requirement by minimizing the uncertainty of the charge asymmetry after the continuum component is subtracted from the on-peak data. A total of 8.5×10^7 single electrons are selected in the on-peak data, of which approximately 63% are from direct semileptonic B decays. Finally, the single electrons are randomly sampled so that the signal momentum spectrum matches that of the dilepton events.

Raw asymmetries of the single electrons in the on- and off-peak data are found to be $a_{\mathrm{on}} = (4.16 \pm 0.14) \times 10^{-3}$ and $a_{\mathrm{off}} = (11.1 \pm 1.4) \times 10^{-3}$. The larger asymmetry in the off-peak data is primarily due to the radiative Bhabha background and the larger detector acceptance in the backward (positron-beam) direction. The continuum fraction $f_{\mathrm{cont}} = (10.32 \pm 0.02)\%$ is obtained from the ratio of the selected single electrons and the integrated luminosities in off- and on-peak data [12]. The neutral B fraction in the $B\bar{B}$ component $f_{B^0} = (48.5 \pm 0.6)\%$ is the $\Upsilon(4S) \to B^0 \bar{B}^0$ branching fraction [20] corrected for the selection efficiency. The cascade event fractions $f_{B^0}^{\mathrm{casc}} = 19.8\%$ and $f_{D^\pm}^{\mathrm{casc}} = 15.3\%$ are obtained from simulation,
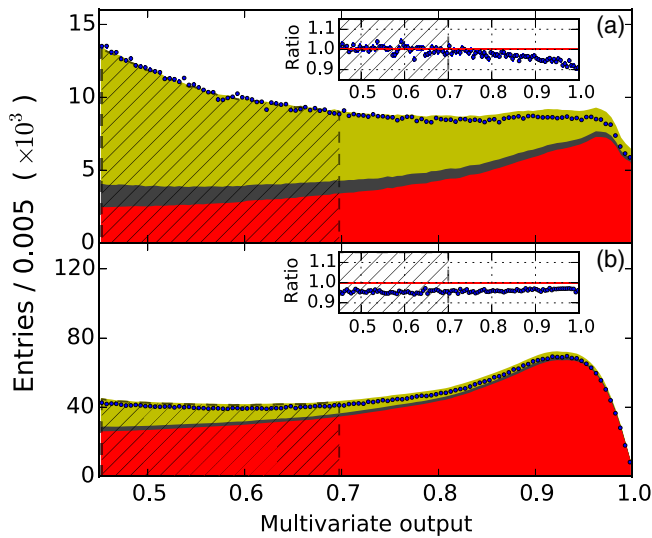

FIG. 1 (color online). Signal probability distributions from the dilepton multivariate algorithm for (a) the same-sign sample and (b) the opposite-sign sample; all lepton flavors are combined. Points are continuum-subtracted data; shaded regions from bottom to top are for signal, $B\bar{B}$ background with ≥ 1 misidentified lepton, and $B\bar{B}$ background with both real leptons. Hatched region is rejected. Data/MC simulation ratios are shown in inset plots. Regions below 0.45 are not shown.

TABLE I.   Continuum-subtracted number of events.

	$\ell^+\ell^+$	$\ell^+\ell^-$	$\ell^-\ell^+$	$\ell^-\ell^-$
ee	$82\,303 \pm 320$	$426\,296 \pm 783$	$425\,309 \pm 782$	$81\,586 \pm 323$
$e\mu$	$55\,277 \pm 263$	$384\,552 \pm 684$	$378\,261 \pm 660$	$55\,878 \pm 264$
μe	$67\,399 \pm 290$	$467\,591 \pm 737$	$475\,363 \pm 744$	$67\,152 \pm 290$
$\mu\mu$	$47\,384 \pm 243$	$277\,936 \pm 619$	$278\,691 \pm 618$	$48\,145 \pm 247$

with negligible statistical uncertainties. The fraction of the misidentified electron is 0.19%, and the asymmetry is approximately 35%. The difference between direct and cascade electron asymmetries is $(-1.16 \pm 0.25) \times 10^{-3}$ in MC simulation. The probability $w_{B^0}^{\text{casc}}$ in MC simulation is found to be $(73.8 \pm 0.1)\%$. Using these numerical values, we determine the coefficients in Eq. (6): $a_{\text{on}} - \alpha = (2.60 \pm 0.20) \times 10^{-3}$, $\beta\chi_d = 0.057 \pm 0.001$, and $\gamma = 0.8951 \pm 0.0002$.

The fitting procedure is tested on the $B\bar{B}$ MC sample; the result $A_{CP}^{\text{MC}} = (-1.00 \pm 1.04) \times 10^{-3}$ is consistent with the CP-symmetric simulation model. We artificially create a nonzero A_{CP} by reweighing mixed events in the MC sample and confirm that the fitting procedure tracks the change in the A_{CP} without bias. The continuum-subtracted event yields are shown in Table I and are used in Eqs. (4) and (5) for the fit. The result of the fit to data, after correcting for the small bias (-1.0×10^{-3}) in the simulation, is $A_{CP} = (-3.9 \pm 3.5) \times 10^{-3}$, $a_{e_1} = (3.4 \pm 0.6) \times 10^{-3}$, $a_{e_2} = (3.0 \pm 0.6) \times 10^{-3}$, $a_{\mu_1} = (-5.6 \pm 1.1) \times 10^{-3}$, and $a_{\mu_2} = (-6.5 \pm 1.1) \times 10^{-3}$. The remaining free parameters are $N^0_{\ell_1\ell_2}$ and $\chi_d^{\ell_1\ell_2}$. The χ^2 value is 6.2 for 4 degrees of freedom. The correlations between A_{CP} and a_{e_1}, a_{e_2}, a_{μ_1}, and a_{μ_2} are -0.41, -0.47, -0.54, and -0.51, respectively. Correlations among other parameters are negligible. Figure 2 shows the fit results for the six data-taking periods and the four flavor subsamples.

The systematic uncertainties are summarized in Table II. The branching fractions in the B decay chain partially determine the background-to-signal ratio. We correct the MC samples so that important branching fractions are consistent with the world average [20]. These branching
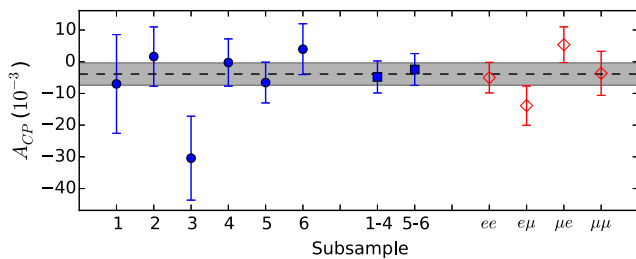
fractions correspond to inclusive B semileptonic decays, $B \to \tau\nu_\tau X$, charm production (D^0, $\bar{D}^0$, $D^\pm$, $D_s^\pm$, Λ_c^+, and $\bar{\Lambda}_c^-$) from B decays, and inclusive charm semileptonic decays. The corrections vary for most decays between 0.57 and 1.32, depending on the channel. We estimate the systematic uncertainty by varying the corrections over their uncertainties, which are dominated by the errors of the world averages.

The systematic uncertainties due to misidentified leptons are estimated by varying the uncertainties of the corrections to e^+, e^-, μ^+, and μ^- individually, and separately for the dilepton and single-electron samples.

In the single-electron MC sample, the charge asymmetry of the electron in $B^0\bar{B}^0$ is slightly different from that in B^+B^- by $(0.46 \pm 0.18) \times 10^{-3}$. Since we cannot separate B^+B^- electrons from $B^0\bar{B}^0$ electrons in the data, the single-electron asymmetry measurement is the average of the two asymmetries, which is half the difference away from the $B^0\bar{B}^0$ electron charge asymmetry. The systematic uncertainty is determined by the change in A_{CP} after shifting the asymmetry in the signal component of the single-electron sample by half the charge asymmetry difference.

The difference in charge asymmetry between the direct and the cascade electrons is found to be $a_e^{\text{casc}} - a_e^{\text{dir}} = (-1.16 \pm 0.25) \times 10^{-3}$ in the single-electron MC sample. The difference between the lower-momentum and the higher-momentum electron asymmetries is negative. This trend is consistent with the result of the fit to the dilepton data: $a_{e_2} - a_{e_1} = (-0.4 \pm 0.7) \times 10^{-3}$. For muons, the corresponding values are $a_\mu^{\text{casc}} - a_\mu^{\text{dir}} = (-0.47 \pm 0.28) \times 10^{-3}$ and $a_{\mu_2} - a_{\mu_1} = (-0.9 \pm 1.2) \times 10^{-3}$. In each case, we set the cascade lepton charge asymmetry to that of the direct lepton and use the change in A_{CP} as a systematic uncertainty.

The background-to-signal ratios $R_{\ell_1\ell_2}^{\pm\pm}$ and $R_{\ell_1\ell_2}^{\pm\mp}$ (under the condition $A_{CP} = 0$) in the dilepton sample are determined from the MC sample. The correction for the misidentified lepton background has been dealt with above. The real lepton portion of the ratio is in principle the same between $\ell^+\ell^+$ and $\ell^-\ell^-$ samples because the particle identification efficiencies cancel between the background

FIG. 2 (color online). A_{CP} of the six data-taking periods (dots), the first four and the last two periods (squares), and the four flavor subsamples (rhombuses). The horizontal band is the $\pm 1\sigma$ region of the final fit result. All error bars are statistical only.

TABLE II.   Summary of systematic uncertainties on A_{CP}.

| Source	(10^{-3})
Generic MC bias correction	1.04
MC branching fractions	0.43
Misidentified lepton corrections in dilepton events	0.77
Misidentified e correction in single electron events	0.65
Difference between neutral and charged B	0.74
Asymmetry difference between direct and cascade e	0.44
Asymmetry difference between direct and cascade μ	0.34
Background-to-signal ratios	0.68
Random forest cut efficiency	0.08
Total	1.90
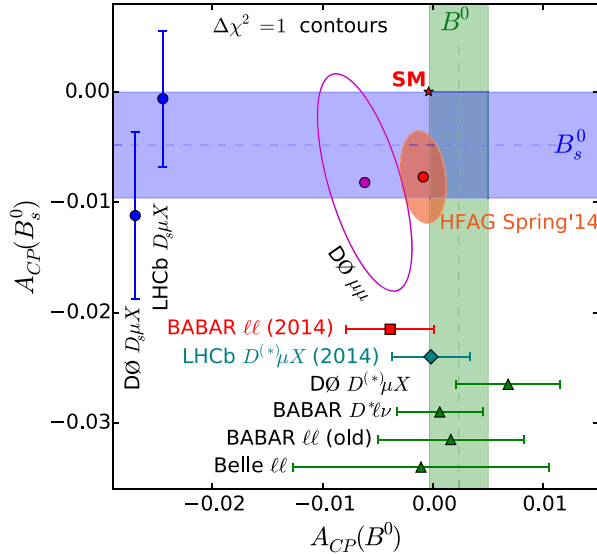
FIG. 3 (color online). Measurements of CP asymmetry in neutral B mixing, including this measurement (red square), recent LHCb result [8] (teal rhombus), Refs. [4–7] (B^0, green triangles), Refs. [21,22] (B_s^0, blue dots), and Ref. [9] (B^0, B_s^0 mixture, magenta contour). The vertical band is the average of Refs. [4–7] and several other older measurements (not shown). The horizontal band is the average of Refs. [21,22]. The 2014 average "HFAG Spring '14" [3] (excluding LHCb [8] and this result) is also shown (orange contour).

and the signal. In the MC sample, they are consistent within 1σ. Varying $R_{\ell_1\ell_2}^{++}$ and $R_{\ell_1\ell_2}^{--}$ or $R_{\ell_1\ell_2}^{+-}$ and $R_{\ell_1\ell_2}^{-+}$ simultaneously in the same direction results in negligible changes in A_{CP}. If they are varied independently, the quadratic sum of the changes in A_{CP} is larger. We use the latter as a systematic uncertainty.

The random forest output distribution in the data could be different from that in the MC sample. The selection efficiency in the MC $B\bar{B}$ dilepton events is approximately 2% larger than that in the data. We move the dilepton random forest selection for the MC sample, while keeping data the same, so that the selected MC events are reduced by up to 6%. We take the average change in A_{CP} as a systematic uncertainty.

Several other sources of systematic uncertainties are studied and found to be negligible. These include the overall dilepton signal fraction estimate, the kinematic difference between on-peak and off-peak data due to different c.m. energies, the continuum component fraction, the probability $w_{B^0}^{\text{casc}}$, the neutral-to-charged B ratio, the same-sign background dilution factors $\delta_{\ell_1\ell_2}$, and the overall cascade event fraction.

In conclusion, we measure the CP asymmetry $A_{CP} = (-3.9 \pm 3.5 \pm 1.9) \times 10^{-3}$ in B^0-$\bar{B}^0$ mixing using inclusive dilepton decays. This result is consistent with the SM prediction and the world average [3]. This measurement represents a significant improvement with respect to our previous result [4] (superseded by this result), and is among the most precise measurements [8,20]. A comparison of experimental results and averages is shown in Fig. 3.

[a]Now at: University of Tabuk, Tabuk 71491, Saudi Arabia.
[b]Also at: Università di Perugia, Dipartimento di Fisica, I-06123 Perugia, Italy.
[c]Now at: Laboratoire de Physique Nucléaire et de Hautes Energies, IN2P3/CNRS, F-75252 Paris, France.
[d]Now at: University of Huddersfield, Huddersfield HD1 3DH, United Kingdom.
[e]Deceased.
[f]Now at: University of South Alabama, Mobile, Alabama 36688, USA.
[g]Also at: Università di Sassari, I-07100 Sassari, Italy.
[h]Also at: INFN Sezione di Roma, I-00185 Roma, Italy.
[l]Now at: Universidad Técnica Federico Santa Maria, 2390123 Valparaiso, Chile.

[1] J. Christenson, J. Cronin, V. Fitch, and R. Turlay, Phys. Rev. Lett. **13**, 138 (1964); D. E. Dorfan, J. Enstrom, D. Raymond, M. Schwartz, S. Wojcicki, D. Miller, and M. Paciotti, *ibid.* **19**, 987 (1967); S. Bennett, D. Nygren, H. Saal, J. Steinberger, and J. Sunderland, *ibid.* **19**, 993 (1967).
[2] A. Lenz, U. Nierste, J. Charles, S. Descotes-Genon, A. Jantsch, C. Kaufhold, H. Lacker, S. Monteil, V. Niess, and S. T'Jampens, Phys. Rev. D **83**, 036004 (2011); A. Lenz and U. Nierste, arXiv:1102.4274.
[3] Y. Amhis et al. (Heavy Flavor Averaging Group), arXiv:1207.1158 and online update http://www.slac.stanford.edu/xorg/hfag/osc/spring 2014/.
[4] B. Aubert et al. (*BABAR* Collaboration), Phys. Rev. Lett. **96**, 251802 (2006).
[5] J. Lees et al. (*BABAR* Collaboration), Phys. Rev. Lett. **111**, 101802 (2013).
[6] V. M. Abazov et al. (D0 Collaboration), Phys. Rev. D **86**, 072009 (2012).
[7] E. Nakano et al. (Belle Collaboration), Phys. Rev. D **73**, 112002 (2006).
[8] R. Aaij et al. (LHCb Collaboration), arXiv:1409.8586.
[9] V. M. Abazov et al. (D0 Collaboration), Phys. Rev. D **89**, 012002 (2014).
[10] V. A. Kostelecky, Phys. Rev. D **64**, 076001 (2001).
[11] B. Aubert et al. (*BABAR* Collaboration), Phys. Rev. D **70**, 012007 (2004).

[12] J. Lees *et al.* (*BABAR* Collaboration), Nucl. Instrum. Methods Phys. Res., Sect. A **726**, 203 (2013).

[13] D. Lange, Nucl. Instrum. Methods Phys. Res., Sect. A **462**, 152 (2001).

[14] S. Agostinelli *et al.* (GEANT4 Collaboration), Nucl. Instrum. Methods Phys. Res., Sect. A **506**, 250 (2003).

[15] B. Aubert *et al.* (*BABAR* Collaboration), Nucl. Instrum. Methods Phys. Res., Sect. A **479**, 1 (2002); **729**, 615 (2013).

[16] See Supplemental Material at http://link.aps.org/supplemental/10.1103/PhysRevLett.114.081801 for the detailed derivation of the equation.

[17] G. C. Fox and S. Wolfram, Phys. Rev. Lett. **41**, 1581 (1978).

[18] L. Breiman, Mach. Learn. **45**, 5 (2001).

[19] D. Boutigny *et al.* (*BABAR* Collaboration), Report No. SLAC-R-504, edited by P. F. Harrison and H. R. Quinn, 1998, Chap. 4.

[20] J. Beringer *et al.* (Particle Data Group), Phys. Rev. D **86**, 010001 (2012).

[21] V. Abazov *et al.* (D0 Collaboration), Phys. Rev. Lett. **110**, 011801 (2013).

[22] R. Aaij *et al.* (LHCb Collaboration), Phys. Lett. B **728**, 607 (2014).